System Level 5G Evaluation of MIMO-GFDM in an LTE-A Platform

Ghaith Al-Juboori, Angela Doufexi and Andrew R. Nix
Communication Systems and Networks Group-Department of Electrical and Electronic Engineering
University of Bristol, Bristol, United Kingdom.
Email: Ghaith.al-juboori, a.doufexi, Andy.nix@bristol.ac.uk

***Abstract*—The 5G physical layer will support applications with different requirements, such as high data rate, ultra low power consumption and low latency. Recently, there is significant interest in the design and performance of new waveforms for 5G. One of the most important candidates is the Generalised Frequency Division Multiplexing (GFDM) waveform. The new waveform must support a smooth transition from current 4G solutions. In this paper, the performance of MIMO-GFDM with spatial multiplexing is studied in the context of LTE-A using the 3D 3GPP-ITU channel model. Additionally, results are compared with corresponding OFDM solutions. Our investigations illustrate that GFDM achieves comparable performance (Packet Error Rate (PER) and throughput), while offering additional gains such as decreased out-of-band radiation, which is a key factor for many 5G applications such as M2M and IoT.**

***Keywords*—GFDM; MIMO; OFDM; LTE-A.**

I. INTRODUCTION

5G will support a number of applications such as Machine Type Communications (MTC), Internet of Things (IoT) and mobile communications. In order to achieve these different requirements, varied technologies will be deployed such as Massive MIMO, high frequency bands (millimetre wave signals) and new waveforms in the physical layer. The selection of new waveforms is key due to its effect on transceiver complexity [1].

OFDM has desirable features such as its immunity against Inter-Symbol Interference (ISI) and modest implementation complexity using Fast Fourier Transform (FFT) algorithms. OFDM is employed in many standards and applications such as the 4G cellular mobile standards (LTE & LTE-A) [2]. On the other hand, OFDM has several drawbacks that may prevent it from being used in 5G, for example, high Out-Of-Band (OOB) radiation, sensitivity to time and frequency synchronisation and a high Peak to Average Power Ratio (PAPR) [3].

Recent research in 5G waveforms has focused fundamentally in two directions. The first direction has suggested enhancements and alternatives to the OFDM waveform to improve its properties, such as its sensitivity to carrier frequency offset and spectral containment [4]. The second direction is to replace OFDM with another waveform. Many waveforms have been suggested such as Filter Bank Multi-Carrier (FBMC) [5], Universal Filter Multi-Carrier (UFMC) [6] and GFDM [1]. In this paper, the system level performance of MIMO-GFDM, using spatial multiplexing, is evaluated and compared with OFDM waveforms for a multi-cell LTE-A like 5G deployment.

The remainder of this paper is arranged as follows: Section II provides a brief description of GFDM and the MIMO-GFDM system model. Section III lists the simulation parameters used for LTE-A, GFDM based LTE-A and the system level studies respectively. In section IV, the simulation results are shown and discussed. Conclusions are given in section V.

II. SYSTEM MODEL OVERVIEW

Due to its flexibility to address the different requirements of 5G, GFDM is proposed as one of the digital multicarrier modulation scheme candidates for 5G. The complex-value data vector is distributed over M sub-symbols and K sub-carriers within one GFDM block. Unlike OFDM, GFDM has M sub-symbols per sub-carrier and the pulse shape filtering process is performed per sub-carrier to reduce the OOB radiation. As mentioned in [7], orthogonal and non-orthogonal filters can be used as a prototype filter in the filtering process, which increases the flexibility of GFDM. An up-conversion step, which implies the shifting of each sub-carrier to the appropriate position is performed prior to adding all the sub-carrier signals together to form the final GFDM signal, which can be written as:

$$x[n] = \sum_{k=0}^{K-1} \sum_{m=0}^{M-1} g_{k,m}[n] d_{k,m}, \tag{1}$$

where $d_{k,m}$ is the data symbol to be transmitted on the m^{th} sub-symbol and the k^{th} sub-carrier of the GFDM block, and $g_{k,m}$ describes the time and frequency shifted versions of the prototype filter and can be written as:

$$g_{k,m}[n] = g[(n - mK) mod N] e^{-j2\pi \frac{k}{K} n}, \tag{2}$$

where n represents the sampling index (from 0 to N-1) and N is equal to $K \times M$. To reduce the computation complexity of GFDM implementation, the method mentioned in [3] is used in this paper. A 2 by 2 MIMO-GFDM system in the spatial multiplexing mode is considered and the transmit power is equally distributed over both antennas due to the assumption that no Channel State Information (CSI) is available at the transmitter. The transmitter architecture is depicted in Fig. 1 [8].

The signal at the receiving antennas can be written as:

$$\vec{\mathbf{y}} = \mathbf{H}\vec{\mathbf{s}} + \vec{\mathbf{n}}, \tag{3}$$

where $\vec{\mathbf{s}}$ is the transmit signal vector, $\vec{\mathbf{s}} = [\vec{\mathbf{s_1}}, \vec{\mathbf{s_2}}]^{\mathbf{T}}$ and $\vec{\mathbf{s_i}}$ is the GFDM signal after adding the Cyclic Prefix (CP) at antenna 'i'. $\mathbf{H}$ represents the equivalent channel of the MIMO

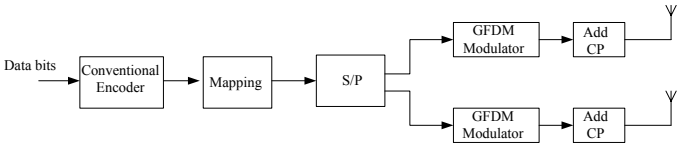

Fig. 1. MIMO-GFDM transmitter architecture.

TABLE I. GENERAL PARAMETERS FOR LTE-A SYSTEM.

Parameter	Value
Sub-frame Duration	1 msec. -30,720 samples
Slot Duration	0.5 msec.
Sub-carrier Spacing	15 kHz
Sampling Frequency	30.72 MHz
No. of Total Sub-carriers	2048
No. of Active Sub-carriers	1200
No. of OFDM per Sub-frame	14 (One packet)
CP Length -First Symbol	160
CP Length- Other Symbols	144
Channel Coding	Turbo Code
MCS Modes	QPSK 1/3,QPSK 1/2,QPSK2/3 16QAM 1/2, 16QAM 2/3 16QAM 4/5, 64QAM 2/3 64QAM 3/4, 64QAM 4/5

system. The signal at the receiving antennas is $\vec{\mathbf{y}} = [\vec{\mathbf{y_1}}, \vec{\mathbf{y_2}}]^{\mathbf{T}}$, where $\vec{\mathbf{y_j}}$ is the received signal at antenna 'j' and $\vec{\mathbf{n}}$ represents AWGN with a variance denoted by σ^2. In this paper, a Linear Minimum Mean Square Error (LMMSE) detector is used at the receiver. Moreover, the Zero Forcing (ZF) method is used to implement the GFDM demodulator due to its simplicity and resilience to performance loss due to noise enhancement when an orthogonal filter is used [9].

III. SIMULATION PARAMETERS

A. LTE-A Parameters

A Monte-Carlo simulation method was used to simulate a 20MHz FDD LTE-A downlink. The LTE-A system parameters are listed in Table I [10]. The standard mode for LTE-A, in which the CP length for the first and the subsequent symbols are 160 and 144 samples respectively, was used.

B. GFDM Based LTE-A Parameters

Table II lists the parameters that were used to implement the GFDM based LTE-A system [9]. In this system, the GFDM symbol duration is chosen to be an integer part of the LTE-A sub-frame, which is equal to 1 msec. Additionally, a group of its sub-carriers are placed into a multiple number of LTE-A resource blocks (each resource block equal to 180 kHz). The other parameters that are not mentioned in the Table II, such as the channel coding and the MCS are the same as in Table I.

TABLE II. GFDM BASED LTE-A PARAMETERS.

Parameter	Value
Sub-frame Duration	1 msec. -30,720 samples
GFDM Symbol Duration	66.67 sec. or 2048 samples
Sub-Symbol Duration	4.17sec or 128 samples
Sampling Frequency	30.72 MHz
No. of Total Sub-carriers (K)	128
No. of Active Sub-carriers(Kon)	75
Sub-carrier Spacing	240kHz
No. of Sub-symbols per GFDM Symbol (M)	15
No. of GFDM Symbols per Sub-frame	15 (One packet)
CP Length	4.17sec or 128 samples
Prototype Filter	Dirichlet

TABLE III. SYSTEM LEVEL STUDY PARAMETERS.

Parameter	Value
Channel Model	Extended 3D 3GPP-ITU channel model [13]
PDSCH Simulation Model	MIMO 2 by 2bit level simulator
Bandwidth	20 MHz
Carrier frequency	2.6GHz
Environment	Urban-Macro
Main BS-UE distance	50-1000 m
Cell Radius	500 m
BS Transmit Power	43 dBm
No. of UE per cell	900
BS Antenna Height	25m
BS down tilt	10
Min. UE Sensitivity	-120 dBm
Link Direction	Downlink (from BS to UE)
Noise Figure	9 dB
BS Antenna Type	Measured patch antennas as in [14]
UE Antenna Type	Measured hand set antenna as in[14]

C. System-Level Parameters

In this work, the 3GPP macro cellular deployment model with a frequency reuse factor of 1 is used as shown in Fig. 2. In this model each cell contains three sectors and the cell radius, cell diameter and the Inter Site Distance (ISD) are R, 2R and 3R respectively [11].

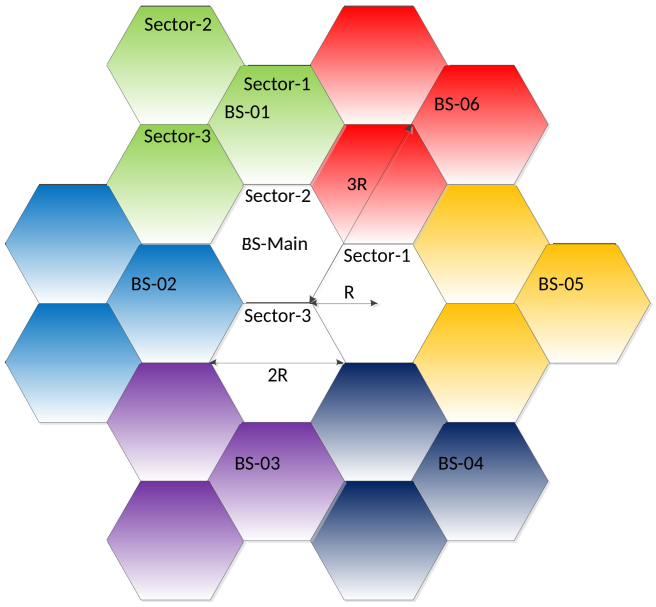

Fig. 2. 3GPP three sector cell deployment [12].

A bit level simulator for both OFDM and GFDM based LTE-A systems has been developed and used to quantify each users' performance (Throughput and PER) for different MCS modes. Nine-hundred UEs have been randomly distributed at street level in the main cell; all other system level study parameters are summarised in Table III. In order to get statistically relevant performance data, for each UE, one-thousand channel snapshots were generated for each link (between each UE and the main BS and the other six first-tier interfering BSs). Table IV lists the MCS modes used in this study and also the maximum error free throughput for each mode for both waveforms. Two cases are considered in this paper, namely with and without interference. In the interference free case, the interference from other BSs is neglected and only thermal

TABLE IV. R_{MCS} VALUES FOR BOTH WAVEFORMS AS A FUNCTION OF MCS MODE.

MCS-No.	No. of Bits per Symbol	Coding Rate (Rc)	OFDM -R$_{MCS}$ in Mbps	GFDM -R$_{MCS}$ in Mbps
MCS-1	2	1/3	22.4	22.5
MCS-2	2	1/2	33.6	33.75
MCS-3	2	2/3	44.8	45
MCS-4	4	1/2	67.2	67.5
MCS-5	4	2/3	89.6	90
MCS-6	4	4/5	107.52	108
MCS-7	6	2/3	134.4	135
MCS-8	6	3/4	151.2	151.88
MCS-9	6	4/5	161.28	162

noise is considered. The SNR, in this case, is computed as:

$$SNR_{i,M} = \frac{P_{i,Main}}{P_{AWGN}}. \quad (4)$$

$P_{i,Main}$ is the total received power from the main BS sector at a certain UE 'i', while P_{AWGN} is the AWGN power. On the other hand, in the interference case, the interference effect from the different sectors of the six first-tier interfering BSs is also considered. The SINR value for each UE, in this case, is calculated as:

$$SINR_i = \frac{P_{i,Main}}{P_{AWGN} + \sum_{ISI} P_{i,ISI}}, \quad (5)$$

where $P_{i,ISI}$ is the total interference power at the UE 'i'. The throughput for each UE is determined based on the following equation [15].

$$THR_{i,MCS} = R_{MCS}(1 - PER_{i,MCS}) \quad (6)$$

R_{mcs} represents the maximum data rate that can be transmitted without error for a certain MCS mode.

IV. RESULTS

A. Comparison for Different Channel Models

Fig. 3 illustrates the PER versus SNR performance (for more information about the parameters refer to section III) of both waveforms for three different modulation schemes (MSC1, MCS4 and MCS7) in a wide band Rayleigh channel model. This model assumes an exponential Power Delay Profile (PDP) from 0 to -10 dB and 16 taps, as described in [1], [16]. It is clear that the performance of both waveforms is similar.

Additionally, Fig.4 shows the performance of a certain UE in the realistic urban channel scenario using the proposed channel model (see Table III). This UE has a K-factor value of -9.8 dB and delay spread of 0.42 μsec. It is clear that the performance of the two waveforms is very close at low modulation orders (low MCS). On the other hand, OFDM slightly outperforms GFDM at high modulation orders (higher MCS) with a maximum difference of 1 dB seen at high SNR. The reason for this result is that each sub-carrier, in the GFDM case, consists of M samples, therefore, the impact of one sample reflects on M symbols. On the other hand, each frequency sample (sub-carrier) impacts only one symbol of data in the OFDM case [12]. Moreover, the increase of the modulation order (the number of bits in one sample) makes the situation worse for both schemes.

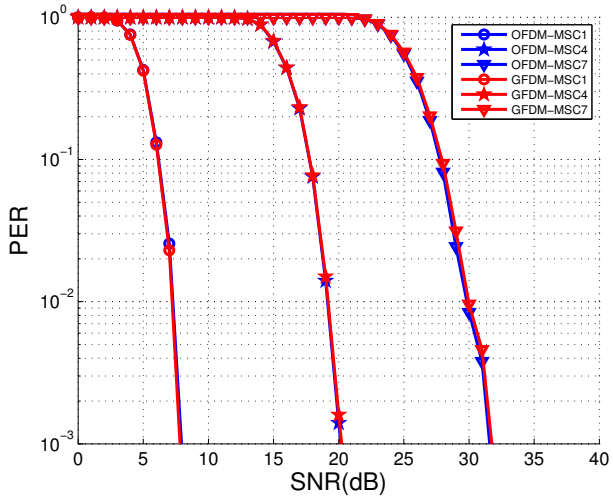

Fig. 3. Waveform performance in a wide-band Rayleigh channel.

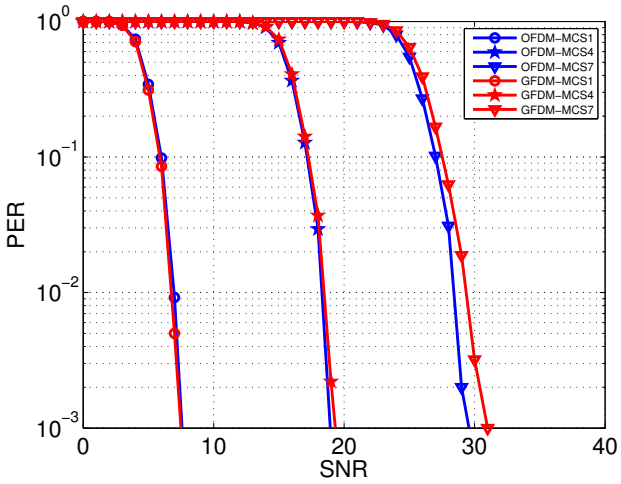

Fig. 4. Waveform performance of a certain UE in a realistic channel scenario.

B. System-Level Analysis

The Cumulative Distribution Function (CDF) of the UEs' SNR and SINR in the centre cell is shown in Fig. 5. It is clear that 60% of the UEs' SNR values are less than or equal to 20 dB. On the other hand, when considering interference from the other adjacent cells, around 60% of the UEs' SINR become less or equal to 2.5 dB. Interference has a dramatic impact on the UEs performance and methods such as beamforming can be used to reduce these effects [17].

The CDF for the PHY throughput for both waveforms, with and without interference, is shown in Fig. 6. Adaptive MCS selection was assumed, where the best MCS for each UE is chosen. As expected, the throughput values in the interference-free case are higher for both waveforms. Around 45% of the UEs have a throughput greater than 40 Mbps in the interference-free case, whereas just 10% of the UEs get this rate when the impact of interference is considered. Moreover, the performance for both waveforms is similar.

Fig. 7 & Fig. 8 show the CDF of the PER for OFDM and

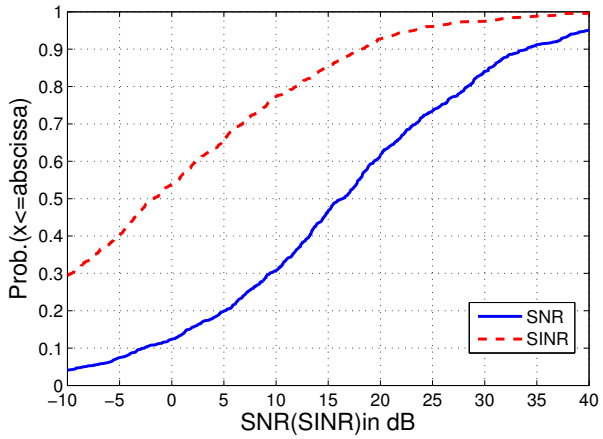

Fig. 5. CDF for the UEs' SNR and SINR.

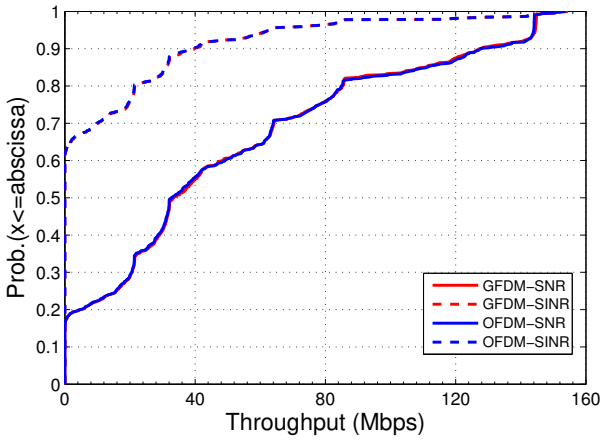

Fig. 6. CDF of the throughput of both waveforms in with and without interference.

GFDM in both cases. It can be seen that their performance is very similar. It is interesting to note that MCS-6 is worse than MCS7 & MCS8 due to the high coding rate R_c.

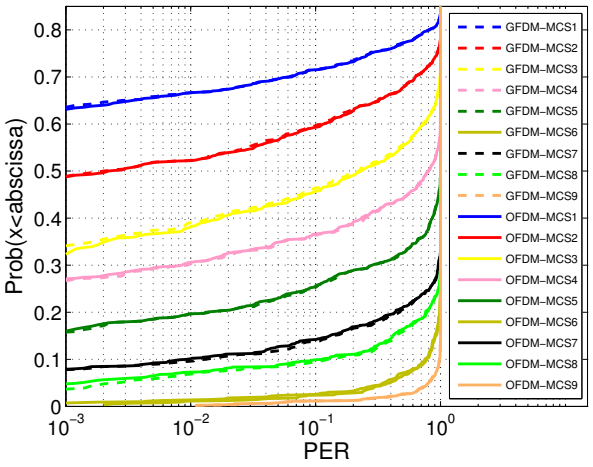

Fig. 7. CDF of the PER of both waveforms in the interference-free case.

Fig. 9 illustrates the PER performance for two UEs (UE-

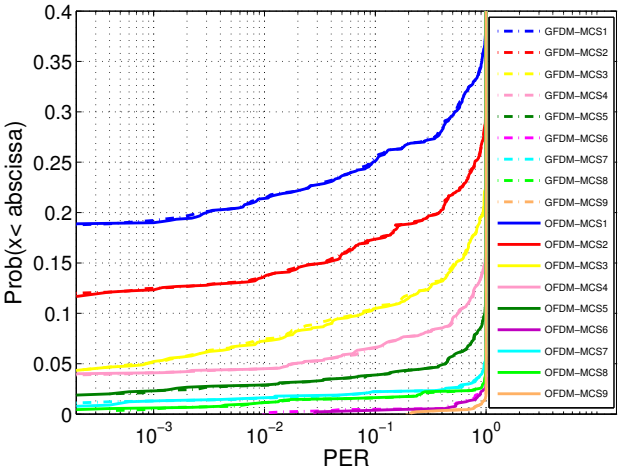

Fig. 8. CDF of the PER of both waveforms in the interference case.

TABLE V. PARAMETERS VALUES FOR TWO SELECTED UES.

UE No.	Tx-Antenna corr. (α)	Rx-Antenna corr. (β)	$\alpha \times \beta$	K-factor (dB)	Delay Spread (μ sec)
4	0.1585	0.1785	0.0283	-9.8	0.42
610	0.7562	0.8107	0.6131	-4.3	0.47

4 & UE-610) which have different spatial correlation values between the transmit and receive antennas. Table V lists the correlation values and other parameters relevant for this scenario. It is clear that UE-4, which experiences low spatial correlation values compared to UE-610, has better performance by 7 dB at a PER level of 1×10^{-3} for both MCS modes (1 & 7). This means the higher the correlation values, the worse the PER performance. This result is due to the fact that spatial correlation between the transmit and receive antennas reduces the theoretic channel capacity [18]. Moreover, the difference between OFDM and GFDM in the high MCS modes reduces for high values of spatial correlation. This means that OFDM is more sensitive to spatial correlation effects than GFDM at high MCS modes.

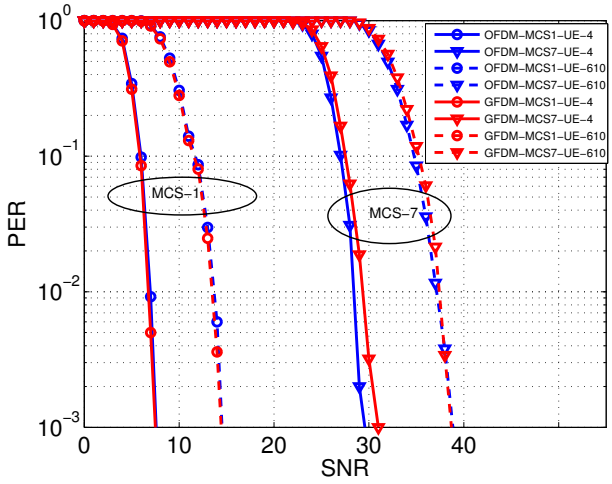

Fig. 9. PER performance of two UEs with different spatial correlation values.

Fig. 10 depicts the Power Spectral Density (PSD) for both waveforms. A reduction of 6 dB in the OOB radiation

can be seen in the GFDM case compared to OFDM. This occurs because both air-interfaces have been forced to deliver similar spectral efficiency ($\frac{N_{cp}}{N}$) [19]. Different methods can be applied to considerably reduce the OOB radiation for GFDM, such as Guard Symbols (GS) and Pinching the Block Boundary (PBB) methods. As shown in Fig. 10, around 20 dB of improvement in the OOB radiation can be obtained when applying the GS method, which implies setting the first and last sub-symbols to a certain value (zero in this paper). Moreover, around 25-45 dB of improvement can be achieved, depending on the window type, when using the PBB method. This involves multiplying the GFDM symbol with certain types of windows (e.g, Ramp and Raised Cosine). However, this gain comes at the cost of reducing the data rate in the first method by a ratio of ($\frac{M-2}{M}$) and enhancing the noise in the second method. For more details about these methods, refer to [1].

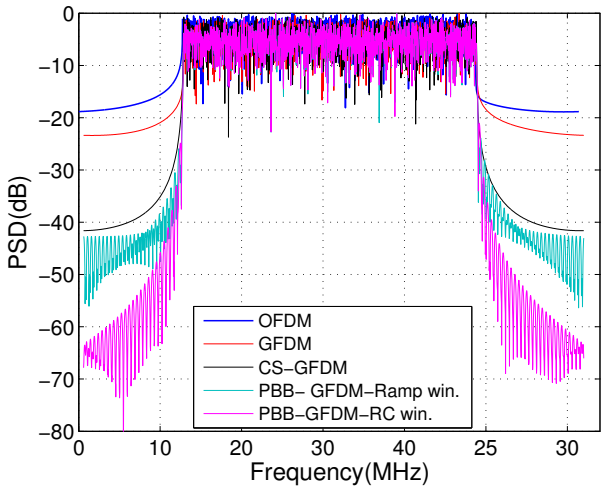

Fig. 10. Power spectral density comparison.

V. CONCLUSION

In this paper, the performance of MIMO-GFDM with spatial multiplexing, for an LTE-A like system has been evaluated and compared with OFDM performance in different channel models. Additionally, a system level study using a realistic channel scenario model (3D 3GPP-ITU) was presented. The simulation results show that the performance of the two waveforms in terms of PER and throughput is similar. Moreover, there is a modest gain in the reduction of OOB radiation in the GFDM case compared to OFDM. However, different methods such as Guard Symbols (GS) & Pinching the Block Boundary (PBB) can be applied for further reduction in the GFDM OOB radiation. Moreover, the effect of spatial correlation between the antennas, for both waveforms, is studied and analysed. GFDM has similar performance to OFDM in terms of PER and throughput but better OOB radiation characteristics. Since GFDM has a low level of OOB radiation compared to OFDM, this feature enables it to be efficiently used in future 5G systems such as cognitive and M2M systems, where low adjacent channel leakage is required.

ACKNOWLEDGEMENT

Ghaith Al-Juboori would like to thank the Higher Committee for Education Development (HCED) in Iraq and the University of Baghdad for sponsoring his Ph.D. studies.

REFERENCES

[1] N. Michailow, M. Matthe, I. S. Gaspar, A. N. Caldevilla, L. L. Mendes, A. Festag, and G. Fettweis, "Generalized frequency division multiplexing for 5th generation cellular networks," *IEEE Transactions on Communications*, vol. 62, no. 9, pp. 3045–3061, 2014.

[2] L. L. Hanzo, Y. Akhtman, L. Wang, and M. Jiang, *MIMO-OFDM for LTE, WiFi and WiMAX: Coherent versus Non-coherent and Cooperative Turbo Transceivers*. John Wiley Sons, 2011, vol. 26.

[3] N. Michailow, I. Gaspar, S. Krone, M. Lentmaier, and G. Fettweis, "Generalized frequency division multiplexing: Analysis of an alternative multi-carrier technique for next generation cellular systems," in *2012 International Symposium on Wireless Communication Systems (ISWCS)*, Aug 2012, pp. 171–175.

[4] G. Berardinelli, K. Pajukoski, E. Lahetkangas, R. Wichman, O. Tirkkonen, and P. Mogensen, "On the Potential of OFDM Enhancements as 5G Waveforms," in *2014 IEEE 79th Vehicular Technology Conference (VTC Spring)*, May 2014, pp. 1–5.

[5] B. Farhang-Boroujeny, "OFDM Versus Filter Bank Multicarrier," *IEEE Signal Processing Magazine*, vol. 28, no. 3, pp. 92–112, May 2011.

[6] V. Vakilian, T. Wild, F. Schaich, S. ten Brink, and J. F. Frigon, "Universal-filtered multi-carrier technique for wireless systems beyond lte," in *2013 IEEE Globecom Workshops (GC Wkshps)*, Dec 2013, pp. 223–228.

[7] N. Michailow, M. Lentmaier, P. Rost, and G. Fettweis, "Integration of a GFDM secondary system in an OFDM primary system," in *Future Network Mobile Summit (FutureNetw), 2011*, Conference Proceedings, pp. 1–8.

[8] J. R. Hampton, "Spatial multiplexing," in *Introduction to MIMO Communications:*. Cambridge: Cambridge University Press, 11 2013, pp. 162–196.

[9] I. Gaspar, L. Mendes, M. Matth, N. Michailow, A. Festag, and G. Fettweis, "LTE-compatible 5G PHY based on generalized frequency division multiplexing," in *2014 11th International Symposium on Wireless Communications Systems (ISWCS)*, Aug 2014, pp. 209–213.

[10] G. T. . V10.4.0, "Evolved universal terrestrial radio access (eutra):physical channels and modulation," Report, December 2011.

[11] G. T. . V10.2.0, "Evolved universal terrestrial radio access (eutra):radio frequency (rf) system scenarios," Report, December 2010.

[12] G. R. Al-Juboori, A. Doufexi, and A. R. Nix, "System level 5G evaluation of GFDM waveforms in an LTE-A platform," in *2016 International Symposium on Wireless Communication Systems (ISWCS)*, Conference Proceedings, pp. 335–340.

[13] R. Almesaeed, A. S. Ameen, E. Mellios, A. Doufexi, and A. R. Nix, "A proposed 3D extension to the 3GPP/ITU channel model for 800 MHz and 2.6 GHz bands," in *The 8th European Conference on Antennas and Propagation (EuCAP 2014)*, April 2014, pp. 3039–3043.

[14] R. Almesaeed, A. S. Ameen, A. Doufexi, and A. R. Nix, "Exploiting the elevation dimension of mimo system for boosting handset capacity," in *2015 IEEE International Conference on Communication Workshop (ICCW)*, June 2015, pp. 1281–1285.

[15] K. C. Beh, A. Doufexi, and S. Armour, "Performance Evaluation of Hybrid ARQ Schemes of 3GPP LTE OFDMA System," in *2007 IEEE 18th International Symposium on Personal, Indoor and Mobile Radio Communications*, Sept 2007, pp. 1–5.

[16] M. Matthe, I. Gaspar, D. Zhang, and G. Fettweis, "Near-ML detection for MIMO-GFDM," in *2015 IEEE 82nd Vehicular Technology Conference (VTC2015-Fall)*, Sept 2015, pp. 1–2.

[17] A. Panagopoulos, *Handbook of Research on Next Generation Mobile Communication Systems*, ser. Advances in Wireless Technologies and Telecommunication:. IGI Global, 2015. [Online]. Available: https://books.google.co.uk/books?id=Tgx4CgAAQBAJ

[18] Y. S. Cho, J. Kim, W. Y. Yang, and C. G. Kang, *MIMO-OFDM Wireless Communications with MATLAB*. Wiley Publishing, 2010.

[19] A. B. Üçüncü and A. Ö. Yilmaz, "Out-of-band radiation comparison of GFDM, WCP-COQAM and OFDM at equal spectral efficiency," *CoRR*, vol. abs/1510.01201, 2015. [Online]. Available: http://arxiv.org/abs/1510.01201